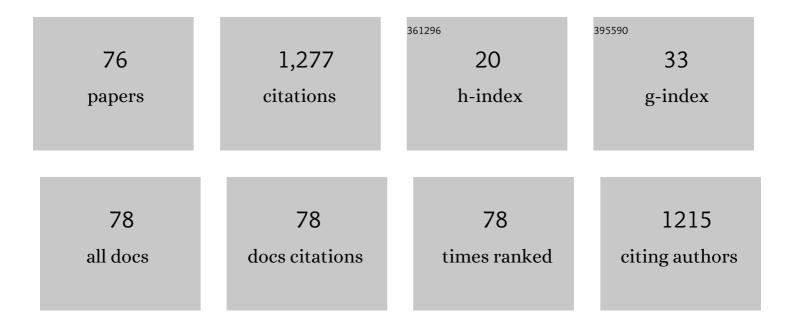
## Chuyang Liu

List of Publications by Year in descending order

Source: https://exaly.com/author-pdf/2068082/publications.pdf Version: 2024-02-01



#	Article	IF	CITATIONS
1	Mineralizer-Assisted Hydrothermal Synthesis and Characterization of BiFeO3Nanoparticles. Journal of the American Ceramic Society, 2007, 90, 2615-2617.	1.9	103
2	Zr <sup>4+</sup> doping-controlled permittivity and permeability of BaFe <sub>12â^x</sub> Zr <sub>x</sub> O <sub>19</sub> and the extraordinary EM absorption power in the millimeter wavelength frequency range. Journal of Materials Chemistry C, 2016, 4, 9532-9543.	2.7	84
3	Exchange coupling controlled ferrite with dual magnetic resonance and broad frequency bandwidth in microwave absorption. Science and Technology of Advanced Materials, 2013, 14, 045002.	2.8	67
4	The tunable magnetic and microwave absorption properties of the Nb <sup>5+</sup> –Ni <sup>2+</sup> co-doped M-type barium ferrite. Journal of Materials Chemistry C, 2017, 5, 3461-3472.	2.7	63
5	Controllable synthesis of nickel nanowires and its application in high sensitivity, stretchable strain sensor for body motion sensing. Journal of Materials Chemistry C, 2018, 6, 4737-4745.	2.7	61
6	Alkali Metal Ions-Assisted Controllable Synthesis of Bismuth Ferrites by a Hydrothermal Method. Journal of the American Ceramic Society, 2007, 90, 3673-3675.	1.9	53
7	Ferroelectric/ferromagnetic ceramic composite and its hybrid permittivity stemming from hopping charge and conductivity inhomogeneity. Journal of Applied Physics, 2013, 113, .	1.1	47
8	Multi-susceptibile Single-Phased Ceramics with Both Considerable Magnetic and Dielectric Properties by Selectively Doping. Scientific Reports, 2015, 5, 9498.	1.6	46
9	Preparation of amorphous calcium phosphate in the presence of poly(ethylene glycol). Journal of Materials Science Letters, 2003, 22, 1015-1016.	0.5	44
10	Highly sensitive hydrogen peroxide biosensors based on TiO2 nanodots/ITO electrodes. Journal of Materials Chemistry, 2012, 22, 9019.	6.7	34
11	Formation of Sol–Gel <i>In Situ</i> Derived <scp>BTO</scp> / <scp>NZFO</scp> Composite Ceramics with Considerable Dielectric and Magnetic Properties. Journal of the American Ceramic Society, 2013, 96, 1240-1247.	1.9	30
12	Enhanced microwave absorption performance of Fe3O4/Cu composites with coexistence of nanospheres and nanorods. Journal of Alloys and Compounds, 2020, 817, 152764.	2.8	30
13	Multiple nature resonance behavior of BaFexTiO19 controlled by Fe/Ba ratio and its regulation on microwave absorption properties. Journal of Alloys and Compounds, 2019, 773, 730-738.	2.8	29
14	Multiferroic Ceramic Composite with In Situ Glassy Barrier Interface and Novel Electromagnetic Properties. Journal of Physical Chemistry C, 2014, 118, 5802-5809.	1.5	28
15	Reduced Graphene Oxide-CoFe <sub>2</sub> O <sub>4</sub> /FeCo Nanoparticle Composites for Electromagnetic Wave Absorption. ACS Applied Nano Materials, 2020, 3, 8939-8948.	2.4	27
16	Percolative NZFO/BTO ceramic composite with magnetism threshold. Journal of Materials Chemistry C, 2013, 1, 6325.	2.7	26
17	Enhanced microwave absorption properties of Zr4+-doped Fe3O4 for coordinated impedance matching and attenuation performances. Journal of Alloys and Compounds, 2019, 790, 316-325.	2.8	26
18	Formation of BaFe <sub>12â^'<i>x</i></sub> Nb <sub><i>x</i></sub> O <sub>19</sub> and its high electromagnetic wave absorption properties in millimeter wave frequency range. Journal of the American Ceramic Society, 2017, 100, 3999-4010.	1.9	25

#	Article	IF	CITATIONS
19	Enhanced microwave absorption properties of barium ferrites by Zr4+-Ni2+ doping and oxygen-deficient sintering. Journal of Magnetism and Magnetic Materials, 2020, 494, 165828.	1.0	23
20	Excellent absorption properties of BaFe <sub>12â^x</sub> Nb <sub>x</sub> O <sub>19</sub> controlled by multi-resonance permeability, enhanced permittivity, and the order of matching thickness. Physical Chemistry Chemical Physics, 2017, 19, 21893-21903.	1.3	22
21	Formation of BaFe12-xNixO19 ceramics with considerably high dielectric and magnetic property coexistence. Journal of Alloys and Compounds, 2018, 765, 951-960.	2.8	22
22	Magnetoelectric coupling tailored by the orientation of the nanocrystals in only one component in percolative multiferroic composites. RSC Advances, 2019, 9, 20345-20355.	1.7	21
23	Initial permeability of percolative PbTiO3/NiFe2O4 composite ceramics by a sol–gel in situ process. Journal of Materials Chemistry, 2010, 20, 10856.	6.7	20
24	Incorporation of chitosan nanospheres into thin mineralized collagen coatings for improving the antibacterial effect. Colloids and Surfaces B: Biointerfaces, 2013, 111, 536-541.	2.5	20
25	Dipole azimuth dependent permittivity in randomly and (100) oriented (Pb,Sr)TiO3 thin films. Journal of Materials Chemistry, 2011, 21, 10808.	6.7	19
26	Broad microwave absorption bandwidth achieved by exchange coupling interaction between hard and soft magnetic materials. Ceramics International, 2021, 47, 2879-2883.	2.3	18
27	Direct Control of Defects on Positron Lifetimes and Dielectric Constant of Microwave Ceramics. Journal of the American Ceramic Society, 2013, 96, 2537-2543.	1.9	17
28	Effect of Pluronic F127 on the pore structure of macrocellular biodegradable polylactide foams. Polymers for Advanced Technologies, 2004, 15, 425-430.	1.6	16
29	Relation between the microstructure and the electromagnetic properties of BaTiO3/Ni0.5Zn0.5Fe2O4 ceramic composite. Applied Physics A: Materials Science and Processing, 2015, 119, 1291-1300.	1.1	16
30	Synthesis of broad microwave absorption bandwidth Zr4+-Ni2+ ions gradient-substituted barium ferrite. Ceramics International, 2020, 46, 25808-25816.	2.3	16
31	Control of the nanostructure in percolative multiferroic composites on the dielectric loss and magnetism threshold. Journal of Materials Chemistry C, 2015, 3, 9076-9088.	2.7	15
32	Azimuthally Controlled Magnetic and Dielectric Properties of Multiferroic Nanocrystalline Composite by Magnetic Coupling and Charge Hopping. Journal of Physical Chemistry C, 2015, 119, 17995-18005.	1.5	15
33	Millimeter-wave absorption properties of BaTiO <sub>3</sub> /Co <sub>3</sub> O <sub>4</sub> composite powders controlled by high-frequency resonances of permittivity and permeability. Journal of Materials Chemistry C, 2018, 6, 12965-12975.	2.7	13
34	A novel and facile route for the <i>in situ</i> formation of composites with dual coupling interactions for considerable millimeter wave absorption performance. Journal of Materials Chemistry C, 2021, 9, 12523-12529.	2.7	12
35	Formation of intercalation compound of kaolinite–glycine via displacing guest water by glycine. Journal of Colloid and Interface Science, 2014, 432, 278-284.	5.0	10
36	Titanium dioxide nanorod-based amperometric sensor for highly sensitive enzymatic detection of hydrogen peroxide. Mikrochimica Acta, 2013, 180, 1487-1493.	2.5	9

#	Article	lF	CITATIONS
37	Formation of nano-Ag/BiFeO3 composite thin film with extraordinary high dielectric and effective ferromagnetic properties. Journal of Materials Science: Materials in Electronics, 2017, 28, 5652-5662.	1.1	9
38	In Situ and Intraoperative Detection of the Ureter Injury Using a Highly Sensitive Piezoresistive Sensor with a Tunable Porous Structure. ACS Applied Materials & amp; Interfaces, 2021, 13, 21669-21679.	4.0	9
39	Shape-controlled synthesis of lead zirconate titanate nanocrystallites, microrods, microrolls and 3D complex architectures via the effects of poly-vinylalcohol macromolecular conformation. CrystEngComm, 2012, 14, 6783.	1.3	8
40	Effect of Ag doping on the formation and properties of percolative Ag/BiFeO3 composite thin film by sol–gel method. Applied Physics A: Materials Science and Processing, 2017, 123, 1.	1.1	8
41	Formation of 0.84 nm Hydrated Kaolinite as an Environmentally Friendly Precursor of a Kaolinite Intercalation Compound. Clays and Clay Minerals, 2013, 61, 416-423.	0.6	7
42	Multi-field susceptible high-f <sub>c</sub> ceramic composite with atypical topological microstructure and extraordinary electromagnetic properties. Journal of Materials Chemistry C, 2014, 2, 7482.	2.7	7
43	Percolative multi-susceptible PVDF/NZFO composite films with triply controlled high dielectric and magnetic properties. Journal of Applied Physics, 2018, 123, .	1.1	7
44	Broadened ferromagnetic resonance range in ferrite by gradient composition design. Ceramics International, 2019, 45, 24900-24902.	2.3	7
45	Achievement of superior microwave absorption performance and ultra-wide regulation frequency range in Fe-Co-Nd via tuning the phase constitution and crystallinity. Journal of Magnetism and Magnetic Materials, 2020, 502, 166561.	1.0	7
46	Facile fabrication of rGO/Zr4+-Ni2+ gradient-doped BaM composites for broad microwave absorption bandwidth. Ceramics International, 2021, 47, 4333-4337.	2.3	7
47	A solid solution-based millimeter-wave absorber exhibiting highly efficient absorbing capability and ultrabroad bandwidth simultaneously <i>via</i> a multi-elemental co-doping strategy. Journal of Materials Chemistry C, 2022, 10, 1381-1393.	2.7	7
48	Percolative nanoparticle-Ag/PbZr0.52Ti0.48O3 composite thin film with high dielectric and ferroelectric properties. Journal of Materials Science: Materials in Electronics, 2015, 26, 448-455.	1.1	5
49	Anisotropy of Percolation Threshold of BaTiO3-Ni0.5Zn0.5Fe2O4 Composite Films. Scientific Reports, 2019, 9, 7855.	1.6	5
50	Investigation of Optimal Photosensor in A-Si:H Liquid Crystal Light Valves. Materials Research Society Symposia Proceedings, 1992, 258, 1175.	0.1	4
51	Synthesis and properties of SDC powders and ceramics for low temperature SOFC by stearic acid process. Journal of Electroceramics, 2008, 21, 698-701.	0.8	4
52	DIELECTRIC BEHAVIOR OF NOVEL ACETYLENE BLACK–PVDF/BaTiO3 TRI-PHASE COMPOSITE FILM. Surface Review and Letters, 2008, 15, 19-22.	0.5	4
53	Effect of Zn doping on structure and ferroelectric properties of PST thin films prepared by sol–gel method. Journal of Materials Science: Materials in Electronics, 2011, 22, 351-358.	1.1	4
54	Control of gradient activation energy on the formation and properties of multiferroic composite thin films. Journal of Materials Chemistry C, 2016, 4, 2028-2039.	2.7	4

#	Article	IF	CITATIONS
55	Selectively doped barium ferrite ceramics with giant permittivity and high tunability under extremely low electric bias. Journal of Applied Physics, 2021, 130, 124101.	1.1	4
56	Characterization of A-Si : H and A-SiGe : H Films in Liquid Crystal Light Valve. Materials Research Society Symposia Proceedings, 1991, 219, 179.	0.1	3
57	Percolative ceramic composites with giant dielectric constants and low dielectric losses. Journal of Materials Chemistry, 2010, , .	6.7	3
58	Tailoring the light absorption of Ag-PZT thin films by controlling the growth of hexagonal- and cubic-phase Ag nanoparticles. Applied Physics A: Materials Science and Processing, 2017, 123, 1.	1.1	3
59	Multimode Signal Processor Unit Based on the Ambipolar WSe <sub>2</sub> –Cr Schottky Junction. ACS Applied Materials & Interfaces, 2019, 11, 38895-38901.	4.0	3
60	A tri-phase percolative ceramic composite with high initial permeability and composition-independent giant permittivity. RSC Advances, 2019, 9, 30641-30649.	1.7	3
61	Control of Oxygen Vacancies in TiO <sub>6</sub> Octahedra of Amorphous BaTiO <sub>3</sub> Thin Films with Tunable Builtâ€in Electric Field in <i>a</i> â€BaTiO <sub>3</sub> / <i>p</i> â€Si Heterojunction for Metal–Oxide–Semiconductor Applications. Physica Status Solidi (A) Applications and Materials Science, 2020, 217, 1900941.	0.8	3
62	Structural Nature of Nanocrystalline Silicon. Materials Research Society Symposia Proceedings, 1993, 297, 381.	0.1	2
63	Effect of Heat Treatment Temperature on the Formation of Ag Nanoparticles in Ag-PbTiO <sub>3</sub> Composite Thin Films. Ferroelectrics, 2009, 387, 161-166.	0.3	2
64	Preparation of Fine-Grained Multiferroic BaTiO3-(Ni0.5Zn0.5) Fe2O4Ceramic Composites. Ferroelectrics, 2009, 387, 175-183.	0.3	2
65	Scaling behavior and variable-range-hopping conduction of localized polarons in percolative BaTiO3-Ni0.5Zn0.5Fe2O4 ceramic composite with colossal apparent permittivity. Journal of Applied Physics, 2020, 128, .	1.1	2
66	Ultrahigh purity CaCO <sub>3</sub> whiskers derived from the enhanced diffusion of carbonate ions from a larger liquid–gas interface through porous quartz stones. CrystEngComm, 2020, 22, 6407-6414.	1.3	2
67	Colloidal spray pyrolysis preparation and characterization of nanocrystalline NiO-SDC composite powders for SOFCs. Journal of Electroceramics, 2008, 21, 702-705.	0.8	1
68	Control of tensile stress on inducing formation and tunability of (100) oriented Pb x Sr1â^'x TiO3 thin films. Applied Physics A: Materials Science and Processing, 2014, 117, 1171-1177.	1.1	1
69	Defect States in Hydrogenated Amorphous Silicon-Sulphur Alloys by ESR and PAS. Materials Research Society Symposia Proceedings, 1991, 219, 593.	0.1	0
70	PREPARATION AND MORPHOLOGY OF POROUS NANOCALCIUM PHOSPHATE/POLY(L-LACTIC ACID) COMPOSITES. International Journal of Nanoscience, 2005, 04, 517-523.	0.4	0
71	Effect of lead on formation and dielectric tunability of (Pbx,Sr1â^'x )0.85Bi0.1TiO3 thin films. Frontiers of Materials Science in China, 2007, 1, 59-64.	0.5	0
72	A study on CSC-derived Ba2Ti9O20 phase formation and its dielectric property. Journal of Materials Science: Materials in Electronics, 2010, 21, 416-420.	1.1	0

#	Article	IF	CITATIONS
73	Preparation of titanium silicide nanowires by APCVD method. , 2010, , .		0
74	Control of Nano Grains and Wide Carbocyclic Layer Space of Forming Active Carbon with Extraordinary Capacitance Characteristics in Supercapacitors. Journal of Physical Chemistry C, 2021, 125, 6570-6584.	1.5	0
75	Mechanism of Doping-Induced Orientation of Magnetic Phase in a Sol–Gel-Derived Ni <sub>0.5</sub> Zn <sub>0.5</sub> Fe <sub>2</sub> O <sub>4</sub> /BaTiO <sub>3</sub> Multiferroic Thin Film with High Magnetoelectric Coupling. Journal of Physical Chemistry C, 2021, 125, 28025-28038.	1.5	0
76	Formation of calcium carbonate nanoparticles through the assembling effect of glucose and the influence on the properties of PDMS. RSC Advances, 2022, 12, 13600-13608.	1.7	0